

RESEARCH ARTICLE

Metabolomic and Lipidomic Analysis of Serum Samples following *Curcuma longa* Extract Supplementation in High-Fructose and Saturated Fat Fed Rats

Fabrice Tranchida^{1*}, Laetitia Shintu^{1*}, Zo Rakotoniaina¹, Léopold Tchiakpe², Valérie Deyris¹, Abel Hiol³, Stefano Caldarelli^{1,4}

1 Aix Marseille Université, Centrale Marseille, Centre National de Recherche Scientifique (CNRS), Institut des Sciences Moléculaires de Marseille (iSm2) Unité Mixte de Recherche (UMR) 7313, Marseille, France, **2** Aix-Marseille Université, Laboratoire de Nutrition-Diététique, Faculté de Pharmacie, Marseille, France, **3** Centre de coopération internationale en recherche agronomique pour le développement (CIRAD), Unité Mixte de Recherche (UMR) QualiSud, Université de La Réunion, Ecole Supérieure d'Ingénieurs Réunion Océan Indien (ESIROI), Saint Denis, France, **4** Institut de Chimie des Substances Naturelles, Unité Propre de Recherche (UPR) 2301, Centre National de Recherche Scientifique (CNRS), Gif-sur-Yvette, France

* fabrice.tranchida@univ-amu.fr (FT); laetitia.shintu@univ-amu.fr (LS)



OPEN ACCESS

Citation: Tranchida F, Shintu L, Rakotoniaina Z, Tchiakpe L, Deyris V, Hiol A, et al. (2015) Metabolomic and Lipidomic Analysis of Serum Samples following *Curcuma longa* Extract Supplementation in High-Fructose and Saturated Fat Fed Rats. PLoS ONE 10(8): e0135948. doi:10.1371/journal.pone.0135948

Editor: Anna Alisi, Bambino Gesù' Children Hospital, ITALY

Received: March 2, 2015

Accepted: July 29, 2015

Published: August 19, 2015

Copyright: © 2015 Tranchida et al. This is an open access article distributed under the terms of the [Creative Commons Attribution License](https://creativecommons.org/licenses/by/4.0/), which permits unrestricted use, distribution, and reproduction in any medium, provided the original author and source are credited.

Data Availability Statement: All relevant data are within the paper and its Supporting Information files.

Funding: The authors received no specific funding for this work.

Competing Interests: The authors have declared that no competing interests exist.

Abstract

We explored, using nuclear magnetic resonance (NMR) metabolomics and fatty acids profiling, the effects of a common nutritional complement, *Curcuma longa*, at a nutritionally relevant dose with human use, administered in conjunction with an unbalanced diet. Indeed, traditional food supplements have been long used to counter metabolic impairments induced by unbalanced diets. Here, rats were fed either a standard diet, a high level of fructose and saturated fatty acid (HFS) diet, a diet common to western countries and that certainly contributes to the epidemic of insulin resistance (IR) syndrome, or a HFS diet with a *Curcuma longa* extract (1% of curcuminoids in the extract) for ten weeks. Orthogonal projections to latent structures discriminant analysis (OPLS-DA) on the serum NMR profiles and fatty acid composition (determined by GC/MS) showed a clear discrimination between HFS groups and controls. This discrimination involved metabolites such as glucose, amino acids, pyruvate, creatine, phosphocholine/glycerophosphocholine, ketone bodies and glycoproteins as well as an increase of monounsaturated fatty acids (MUFAs) and a decrease of n-6 and n-3 polyunsaturated fatty acids (PUFAs). Although the administration of *Curcuma longa* did not prevent the observed increase of glucose, triglycerides, cholesterol and insulin levels, discriminating metabolites were observed between groups fed HFS alone or with addition of a *Curcuma longa* extract, namely some MUFA and n-3 PUFA, glycoproteins, glutamine, and methanol, suggesting that curcuminoids may act respectively on the fatty acid metabolism, the hexosamine biosynthesis pathway and alcohol oxidation. *Curcuma longa* extract supplementation appears to be beneficial in these metabolic pathways in rats. This metabolomic approach highlights important serum metabolites that could help in understanding further the metabolic mechanisms leading to IR.

Introduction

Fructose consumption from corn syrup, a common sweetener used in the food industry, has increased dramatically over the past few decades in industrialized countries, and its impact on health has been recently reviewed [1]. Similarly, the intake of saturated fats has risen during the same time period. It has been reported that these two factors contribute to the epidemic of metabolic syndrome [2,3], which is generally considered to be an association of impaired glucose tolerance, hypertension, dyslipidemia, hyperuricemia and central obesity in human beings and animals [4]. Many studies have shown that insulin resistance (IR) is directly associated with lipid disorders, which induced alterations of insulin action and signalling pathways [5]. Moreover, model animals fed a high fructose and high fat diet experienced an increased production of reactive oxygen species (ROS) and/or reactive nitrogen species (RNS) with impaired antioxidant defences [6]. As a consequence, an imbalance between reactive molecular species and antioxidant defences was observed in the development of insulin resistance, impaired insulin secretion and during late complications of diabetes [7].

During the last decade, the development as metabolic disorder treatments of traditional medicine based on natural products has dramatically increased. In this paper, we were particularly interested in the medicinal potential of *Curcuma longa* (CL), a perennial herb native to southern and southeastern tropical Asia commonly termed as turmeric (Zingiberaceae family). Indeed, CL is widely consumed in these regions as a dietary spice and food-coloring as well as for the prevention and therapy of various illnesses [8]. Despite their low bioavailability, curcuminoids, a group of phenolic compounds that are the major bioactive constituent of turmeric extracts, have been shown to possess helpful antioxidant, anticarcinogenic, anti-inflammatory, hypoglycemic, and hypolipidemic actions in animal models as well as human clinical trials [9]. Furthermore, in rats, curcumin, the major curcuminoid present in turmeric, ameliorates IR and diabetes by increasing the uptake and oxidation of fatty acids and glucose in skeletal muscle [10]. However, all these studies were usually performed using concentrations of curcuminoids much higher than those used in nutritional supplements. Indeed, the effect of these supplements taken at a lower dose has been rarely explored yet [11]. In order to characterize its effects on the metabolism, we chose to analyze serum samples from rat fed diets with high fructose and saturated fatty acids alone (HFS) or with the addition of a curcuma extract (HFS+C) using metabolomic and biochemical approaches. Metabolomics has been successfully applied to highlight markers of metabolic alterations in plasma or serum from high-fat and/or high-carbohydrate (fructose and sucrose) fed rodents using nuclear magnetic resonance (NMR) [12,13], or liquid-chromatography coupled with mass spectrometry (LC-MS) [14]. Herein, metabolites and the FA affected by the HFS diet or the absorption of the curcuma extract were identified using NMR and GC/MS-based metabolomics and lipidomics, respectively. We also measured serum antioxidant capacity and lipid peroxidation in order to assess the oxidative stress level in each serum sample.

To the best of our knowledge, no previous study has used an NMR-based metabolomics approach to evaluate the metabolic consequences in response to exposure to HFS diet in rats in conjunction with an extract of CL to highlight possible beneficial effects of this latter.

Materials and Methods

Reagents

All chemicals used in this study were of the highest grade. Acetyl chloride, 2,6-di-tert-butylp-cresol, butylated hydroxytoluene (BHT), methanol, hexane, the internal (23:0 methyl ester), Trolox (6-hydroxy-2,5,7,8-tetramethyl-chroman-2-carboxyl acid) and AAPH (2,2'-azobis

(2-amidinopropane)dihydrochloride) were purchased from Sigma-Aldrich (Sigma-Aldrich Chimie S.a.r.l, Lyon, France). BHT was added to methanol (50 µg BHT/ml methanol) to prevent fatty acid oxidation. The external standards (fatty acid methyl ester, FAME) were purchased from Supelco 37 component FAME mix (Sigma-Aldrich Chimie S.a.r.l, Lyon, France). The internal standard was dissolved in the methanol-BHT solution at a concentration of 100 µg/ml.

Preparation of the hydro-alcoholic extract of *Curcuma longa*

Powder of the rhizome of CL was provided by Laco SARL (Marseille, France). For the extraction, the rhizome of CL was macerated with hot water (80°C) for 4 h, and the aqueous extract was evaporated under vacuum at 60°C. The rhizome residue was re-extracted with ethanol at 60°C during 2 h, filtered, and evaporated under vacuum. The final extract was a 1:1 mixture of the aqueous and alcohol extracts that was re-dissolved with 2% alcohol and then with 0.9% NaCl for the per os administration.

Experimental animals and diets

All animal protocols were approved by the Animal Ethics Committee of the Faculty of Pharmacy of Aix-Marseille Université (Marseille, France) in agreement with the guidelines of the French Ministry of Food and Agriculture. Thirty young male Sprague Dawley (SD) rats (180–200 g) purchased from Elevage Janvier (Le Genest St Isle, France) were maintained in a temperature-and humidity-controlled environment and fed ad libitum. After one week of adaptation under feeding with standard diet (3.32 kcal/g, SAFE, Augy, France), rats were randomly divided into three groups to receive: (i) standard diet (Control group, n = 6); (ii) high fructose and saturated fatty acids diet (4.3 kcal/g SAFE, Augy, France, HFS group, n = 12); (iii) high fructose and saturated fatty acids diet and hydroalcoholic extract of curcuma 100 mg/kg body weight/day by oral gavage (4.3 kcal/g, HFS + C group, n = 12). Control and HFS groups received the same dose of vehicle (a turmeric free hydroalcoholic solution). The total concentration of curcuminoids in the curcuma extract was 1%, as determined by HPLC. Body weight was monitored weekly. After 10 weeks of treatment, the rats were fasted overnight, anesthetized under the mixture of ketamine and xylazine at 60 mg/kg and 5 mg/kg, respectively, and blood sample was collected from the vena cava. Rats were then euthanized by exsanguination. Samples were then centrifuged for 10 min at 1000 g and sera collected and divided into 2 aliquots prior to storage at -80°C until analysis. Livers were removed and weighed. The composition of each diet is reported in [Table 1](#).

Biochemical analysis of serum

Cholesterolemia, triglyceridemia, glycemia, were quantified by SELARL Laboratoire de Biologie Médicale C. Carboni (Aubagne, France). Insulin concentration was measured using a commercial kit (Eurobio, France). An estimate of IR was determined using the homeostasis model assessment index for insulin resistance (HOMA-IR), which was calculated using the formula [fasting insulin (µU/ml) X fasting glucose (mmol/l)]/R. In our study, R = 87.51 was determined empirically as the divisor producing an average HOMA-IR of 1 in control rats, analogous to the assumptions applied in the development of HOMA-IR in humans [15].

Fatty acids determination by gas chromatography-mass spectrometry

The FAME procedure described previously [16] was applied, using a Thermo Scientific ITQ 700 (Thermo Fisher Scientific) gas chromatography-ion trap spectroscopy equipped with PEG

Table 1. Composition of the diets and fatty acid profile.

Constituents (g/100 g dry weight)	Control diet	HFS diet
Protein	19	19
Methionine	0.3	0.3
Starch	62	–
Sucrose	3	–
Cellulose	5	–
Fructose	–	61.7
Minerals and vitamins	7	7
Choline	0.04	0.04
Lard	–	12
Soybean and fish lipid sources	3.5	–
Main fatty acids (% total fatty acids)		
16:0	15.5	24.6
18:0	traces	13.8
16:1n-7	2.3	2.2
18:1n-9	25	37.9
18:2n-6	48	10.8
18:3n-3	0.5	0.8
∑SFA	17	40.6
∑MUFA	30	46.9
∑PUFA	53	12.5

∑ SFA = total saturated fatty acids, ∑ MUFA = total monounsaturated fatty acids, ∑ PUFA = total polyunsaturated fatty acids.

doi:10.1371/journal.pone.0135948.t001

columns (30 m X 0.25 mm id., 0.25 μm thickness) (DB-FFAP Agilent Technologies, France). Data collection and processing were performed by means of XCALIBUR software, (version 2.0 Thermo Fisher Scientific). The relative amount of each fatty acid (% of total fatty acids) was determined by integrating the area under the peak and dividing the result by the total area for all the fatty acid peaks present in the sample.

Estimation of desaturase activity

The product to substrate ratios of (18:1n-9/18:0) and (16:1n-7/16:0), (20:3n-6/18:2n-6), (20:4n-6/20:3n-6) ratios were used to estimate respectively the activities of desaturases Δ9, Δ6 and Δ5 [17].

Quantification of lipid peroxydation and total antioxidant capacity of serum

Malondialdehyde (MDA) levels were measured by the thiobarbituric assay (TBA), and were taken as an index of lipid peroxidation in serum. The MDA-TBA reaction was carried out by mixing 50 μL of plasma or 50 μL standard solutions (MDA tetrabutylammonium from 0.05 to 1.5 μM) with 10 μL of butylhydroxytoluene (BHT, 10 mM) and 450 μL of TBA solution (25 mM in phosphoric acid (0.3 M)–KOH pH 3.5). Then, the reaction mixtures were homogenized by vortex mixing, and placed into a water bath of 95°C for 30 min. Subsequently, the samples were cooled down on ice for 2 h. The supernatant was collected and injected for analysis on a Merck Hitachi/Lachrom HPLC system (L-7100 pump, L-7612 degasser, D-7000 interface and L-7455 diode array detector) using a Macherey-Nagel C18 150/4 (5μM) column. The sample

solutions were analyzed using the following HPLC conditions: mobile phase of methanol/20 mM pH 6.9 potassium phosphate buffer (3:7, v/v). Samples were analyzed by isocratic elution at 45% mobile phase for 8.0 min. The fluorescence wavelengths used were 532 nm and 553 nm for excitation and emission respectively.

The total antioxidant capacity (TAC) of serum was measured in duplicate by using the oxygen radical absorbance capacity (ORAC) assay [18] on a microplate reader Infinite 200 (Tecan Group Ltd, Männedorf Switzerland).

¹H NMR Spectroscopy

After the biochemical analysis, fifty-four serum aliquots (6 pairs for controls; 11 pairs for HFS group; 9 pairs + 2 independent aliquots for HFS +C group) were available for the NMR analysis. NMR samples were prepared using 200 μ l of serum mixed with 400 μ l of 0.9 g.L⁻¹ saline solution (50% D₂O/H₂O (v/v)). All the 1D ¹H NMR experiments were carried out at 300 K on a Bruker Avance spectrometer operating at 500 MHz for the ¹H frequency using a 5-mm cryoprobe. A first set of spectra was collected using a solvent suppression pulse sequence based on the 1D nuclear Overhauser effect spectroscopy pulse sequence (Trd-90°-t1-90°-tm-90°-Taq) for water suppression (Trd = 2s, tm = 150 ms, t1 = 3 μ s) 64 free induction decays (FID) of 32,768 data points were collected using a spectral width of 10 kHz with an acquisition time of 1.64 s. A second set of spectra was acquired on the same samples using a Carr-Purcell-Meiboom-Gill (CPMG) pulse sequence (Trd-90°- $\{\tau$ -180°- τ]_n-Taq) with presaturation of the water signal during a recycle delay of 2s, with τ = 400 μ s and n = 200, for a total filter delay of 160 ms, and the same other parameters described above. The two sets of spectra are complementary since the fatty acid and macromolecule signals dominate the NOESY spectrum when the CPMG experiment attenuates these large signals to unveil the signals of minor metabolites.

For all the spectra, the FIDs were multiplied by an exponential weighting function corresponding to a line broadening of 0.3 Hz and zero-filled before Fourier transformation. NMR spectra were phased and baseline corrected manually and referenced to the glucose α -anomeric signal (δ = 5.23 ppm).

In order to assign the detected metabolites, ¹H-¹H TOCSY [19] (24 transients, 256 increments, mixing time of 80 ms) and ¹H-¹³C HSQC [20] experiments (64 transients, 256 increments) were performed on one sample from each group.

Data processing

The ¹H 1D NMR spectra were directly exported to AMIX 3.8 software (Bruker Biospin GmbH, Karlsruhe, Germany) and divided into 0.001 ppm-width buckets. In order to remove the effects of possible variations in the water suppression efficiency, the region between 4.20 and 5.00 ppm was discarded as well as the signals at 3.86–3.89, 3.52–3.57, 3.42–3.46 and 1.11–1.15 ppm of propylene glycol, an anaesthetic component. The obtained NMR dataset (54 observations x 6508 buckets) was then normalised to the total spectrum intensity. In order to create a model that will explain the impact of the diets on the whole metabolism of the rat and highlight potential correlation between the metabolome (NMR data) and the lipidome (GC/MS data), we combined the NMR dataset and the relative quantification of fatty acid composition in a unique X-matrix (54 observations x 6529 buckets) that was then subjected to statistical analysis using the software Simca-P 12 (Umetrics, Umeå, Sweden). The relative quantification of the fatty acids was replicated in the X-matrix in order to match the duplication of the NMR spectra.

Statistical analyses

The results of the biochemical analysis and the FA composition of serum are expressed as means \pm Standard Error of the Mean (SEM). Unpaired Student's t-test (if the distribution was normal) or nonparametric test Mann–Whitney U test (if the distribution was non-normal) were used for the biochemical analysis. Differences were considered significant for p -value < 0.05 . The FA composition data for the serum were first analyzed using one-way analysis of ANOVA (for FA values with normal distribution) or Kruskal-Wallis test (for FA values with non-normal distribution), which provide specific information on whether a group mean is significantly different from the others. When statistically significant, these tests were followed by a multiple comparison test (post hoc) that uses critical values from Student's t-distribution after a Bonferroni adjustment in order to minimize the proportion of false positives in multiple comparisons. In our study, pairwise comparisons were performed using the adjusted significant level $\alpha^* = 0.017$, the critical values being given by $t_{(N-k, \alpha^*/2)}$ and $t_{(N-k, 1-\alpha^*/2)}$ with $N = 30$ (number of observations) and $k = 3$ (number of groups). The statistical tests were calculated using Sigma Stat software version 3.11 (Systat Software Inc, San Jose, Calif. United States) and MATLAB v7.4 software (The MathWorks Inc., Natick, Massachusetts, United States) for the biochemical and FA composition data, respectively.

Principal component analysis (PCA) was applied to the X-matrix described above as well as to the X-matrix without replication of the data (matrix of 28 samples and 6529 variables). This method was used to detect intrinsic clusters and outliers within the datasets. The comparison of both PCA models, built with or without replication, was carried out in order to assess the effect of the replication of the fatty acid quantification on the statistical model. Since discrimination was not achieved using PCA, the X-matrix was analyzed using supervised OPLS-DA [21] in which we defined the Y-matrix as the matrix of sample classes, i.e. 0 for the controls, 1 for HFS group and 2 for HFS+C group. Model validation was performed by re-sampling it 999 times under the null hypothesis, that is to say generating models with a randomly permuted Y matrix. The quality of the model was assessed by monitoring changes in goodness-of-fit and predictive statistics, R^2 and Q^2 , between the permuted and the original Y matrices.

Results

Body weight gain and biochemical analysis

After 10 weeks of diet the body weight of HFS, HFS+C and control rats was similar in agreement with previous researches [22,23] while a significant increase of relative liver weight was observed in both HFS groups. Compared to control, high fructose and saturated fatty acids diets were associated with a significant increase of glucose, triglycerides, cholesterol and insulin and HOMA-IR levels (Table 2).

Oxidative stress

ORAC and MDA assays were performed to appreciate the total antioxidant capacity and lipid peroxidation level of the sera. Our results showed a decrease in HFS and HFS+C groups of the ORAC score (-12.5 and -23% respectively) associated with an increase (more than 2 fold) of the MDA concentration (Table 3).

Serum fatty acid (FA) profile

In all experimental groups, the major plasma FA were: palmitic (16:0), palmitoleic (16:1n-7), stearic (18:0), oleic (18:1n-9), cis-vaccenic (18:1n-7), linoleic acid (18:2n-6), arachidonic acid (20:4n-6) and docosahexaenoic acid (22:6n-3 or DHA) (Table 4). The change in FA composition

Table 2. Results of serum biochemical analysis after 10 weeks of diet.

Group	Controls	HFS	HFS+C
Body Weight (g)	435.17 ± 20.74	438.42 ± 31.85	444.75 ± 50.78
Relative liver weight	0.0262 ± 0.0008	0.0310 ± 0.0010**	0.0334 ± 0.0016**
HOMAR-IR	1 ± 0.33	10.79 ± 1.89**	6.97 ± 2.05*
Glucose (g/l)	1.07 ± 0.18	1.82 ± 0.41*	1.80 ± 0.44*
Insulin (µg/l)	0.48 ± 0.13	3.34 ± 0.50*	2.22 ± 0.69*
Triglycerides (g/d)	0.435 ± 0.15	0.878 ± 0.22*	1.114 ± 0.36*
Total cholesterol (g/l)	0.60 ± 0.02	0.68 ± 0.04*	0.66 ± 0.06

Relative liver weight is defined as liver weight divided by body weight. Values are mean ± S.E.M (n = 6–12 rats/group).

*P < 0.05 vs. the control

**P < 0.01 vs. the control.

doi:10.1371/journal.pone.0135948.t002

between the controls and the HFS group was fully described in a previous study [22]. Basically, it was observed in the HFS group an increased activity of the delta-9 (Δ9D) and delta-6-desaturase (Δ6D), and a decrease of the delta-5-desaturase (Δ5D), as seen by the 20:4n-6/20:3n-6 ratio, in addition to the depletion of n-6 polyunsaturated fatty acids (n-6 PUFA), 18:2n-6 and its elongation and desaturation product, 20:4n-6. In addition, HFS dietary loading caused a decrease of n-3 PUFA, alpha linolenic acid (18:3n-3, -70%), eicosapentaenoic acid (20:5n-3 or EPA, -33%) and 22:6n-3 (DHA, -33%). The presence of curcuma in the diet did not modify these tendencies. However, the comparison between HFS and HFS+C groups showed a significant decrease of n-3 PUFA, oleic (18:1n-9), myristoleic (14:1) and nervonic acid (24:1n-9) (-75%, -36% and -36%, respectively), associated with a relevant increase of 14:1n-5 and 18:1n-9 acids (more than 2 fold and +22%, respectively).

¹H NMR spectroscopy of serum samples

A typical example of a ¹H CPMG 1D NMR spectrum of a serum sample from a rat fed with a HFS diet supplemented with curcuma extract is shown in Fig 1 (see S1 Fig for an example of a NOESY 1D spectrum of the same sample) and assignments of metabolites are given in S1 Table.

The spectra of serum samples from HFS+C group are dominated by the signals of glucose and lactate, correlated with the hyperglycemia of the rat under high fructose and fat diet. Signals from propylene glycol, a component from the anaesthetic substance used before the sacrifice of the animals, were at a high concentration in the samples and were not included in the statistical analysis.

Table 3. Measurements of lipid peroxidation, total antioxidant capacity of serum after 10 weeks of diet.

Group	Controls	HFS	HFS+C
MDA ^a (µmol/l)	0.31 ± 0.10	0.80 ± 0.07*	0.81 ± 0.048*
ORAC ^b (µmol Trolox equivalent/l)	2763.6 ± 108.9	2456.4 ± 84.3*	2243.1 ± 103.8*

^a Malondialdehyde

^b oxygen radical absorbance capacity.

Values are mean ± S.E.M (n = 6–12 rats/group).

*p < 0.05 vs. the control.

doi:10.1371/journal.pone.0135948.t003

Table 4. Fatty acid composition of serum.

Fatty acid	Controls	HFS	HFS+C	p-value
C12:0 Lauric acid	0.20 ± 0.05	0.12 ± 0.01	0.12 ± 0.02	0.09
C14:0 Myristic acid	0.83 ± 0.03	0.80 ± 0.05	0.82 ± 0.07	0.94
C14:1n-5 Myristoleic acid	0.13 ± 0.05	0.15 ± 0.02	0.33 ± 0.06 ^a	0.009
C16:0 Palmitic acid	19.07 ± 0.91	19.98 ± 0.25	19.97 ± 0.54	0.49
C16:1n-7 Palmitoleic acid	1.80 ± 0.09	2.60 ± 0.26	2.33 ± 0.38	0.24
C18:0 Stearic acid	24.46 ± 0.87	21.71 ± 1.43	20.46 ± 1.91	0.34
C18:1n-9 Oleic acid	7.73 ± 0.20	17.64 ± 0.92 ^a	21.48 ± 1.30 ^{a, b}	0.0000011
C18:1n-7 <i>cis</i> -Vaccenic acid	2.37 ± 0.11	3.14 ± 0.23	2.77 ± 0.31	0.12
C18:2n-6 Linoleic acid	17.00 ± 0.61	13.09 ± 0.68 ^a	13.26 ± 0.93	0.013
C18:3n-6 gamma Linolenic acid	0.11 ± 0.02	0.16 ± 0.03	0.16 ± 0.07	0.57
C18:3n-3 alpha Linolenic acid	0.40 ± 0.11	0.12 ± 0.02	0.09 ± 0.02 ^a	0.003
C20:0 Arachidic acid	0.60 ± 0.13	0.40 ± 0.03	0.28 ± 0.06 ^a	0.011
C20:1n-9 Gondoic acid	0.56 ± 0.12	0.12 ± 0.02 ^a	0.17 ± 0.03	0.018
C20:3n-6 Dihomo gamma linolenic acid	0.12 ± 0.03	0.52 ± 0.06 ^a	0.41 ± 0.04 ^a	0.0002
C20:4n-6 Arachidonic acid	18.69 ± 1.09	15.02 ± 1.08	14.38 ± 0.76 ^a	0.003
C20:5n-3 Eicosopentaenoic acid	0.30 ± 0.06	0.20 ± 0.03	0.05 ± 0.02 ^{a, b}	0.0001
C22:0 Behenic acid	0.28 ± 0.06	0.23 ± 0.02	0.16 ± 0.03	0.05
C22:4n-6 Adrenic acid	0.86 ± 0.20	0.22 ± 0.02	0.11 ± 0.05 ^a	0.004
C24:0 Lignoceric acid	0.86 ± 0.22	0.90 ± 0.10	0.80 ± 0.12	0.83
C22:6n-3 Docosahexaenoic acid	2.65 ± 0.29	1.77 ± 0.16 ^a	1.14 ± 0.06 ^{a, b}	0.00005
C24:1n-9 Nervonic acid	0.98 ± 0.27	1.11 ± 0.09	0.71 ± 0.07 ^b	0.014
∑ SFA	46.30 ± 1.38	44.06 ± 1.50	42.58 ± 2.15	0.50
∑ MUFA	13.57 ± 0.41	24.73 ± 0.98 ^a	27.79 ± 1.59 ^a	0.0005
∑ PUFA	40.12 ± 1.37	31.21 ± 0.88 ^a	29.60 ± 1.21 ^a	0.0015
∑ PUFA n-3	3.35 ± 0.43	2.08 ± 0.15	1.29 ± 0.06 ^{a, b}	0.000038
∑ PUFA n-6	36.78 ± 1.4	29.13 ± 0.81 ^a	28.32 ± 1.22 ^a	0.0042
Δ 9 C16:1n-7/C16:0	0.09 ± 0.003	0.13 ± 0.01	0.12 ± 0.02	0.314
Δ 9 C18:1n-9/C18:0	0.32 ± 0.007	0.87 ± 0.09 ^a	1.23 ± 0.19 ^a	0.0005
Δ 6 C20:3n-6/C18:2n-6	0.01 ± 0.0005	0.04 ± 0.003 ^a	0.03 ± 0.003 ^a	0.0004
Δ 5 C20:4n-6/C20:3n-6	128.67 ± 13.5	36.35 ± 6.16 ^a	39.24 ± 5.09 ^a	0.0008

Relative fatty acid composition (% of total) and estimated desaturase activities in serum of rats fed control, HFS and HFS+C diets. Values are mean ± S.E.M (n = 6–12 rats/group). Samples were measured in duplicate. ∑ SFA total saturated fatty acids, ∑ PUFA total polyunsaturated fatty acids, ∑ MUFA total monounsaturated fatty acids, Δ estimated desaturase activity.

^a significantly different from control group

^b significantly different from HFS group; after multiple comparison tests and Bonferroni adjustment of the significance level.

doi:10.1371/journal.pone.0135948.t004

Multivariate statistical analysis of serum samples

A principal component analysis based on the correlation matrix was performed on the dataset composed of 6508 NMR variables (“buckets”) and 21 fatty acids in order to detect potential outliers and to highlight sample clustering. The first two principal components score plot explaining 34.5% and 13.5% of the total variance, respectively, is shown in Fig 2. A clear discrimination between the controls and the rats that received the diet enriched in fructose and saturated fat was visible along the PC2 axis, although this model was not capable of discriminating between HFS and HFS+C groups. We also noticed no effect of the replication of the

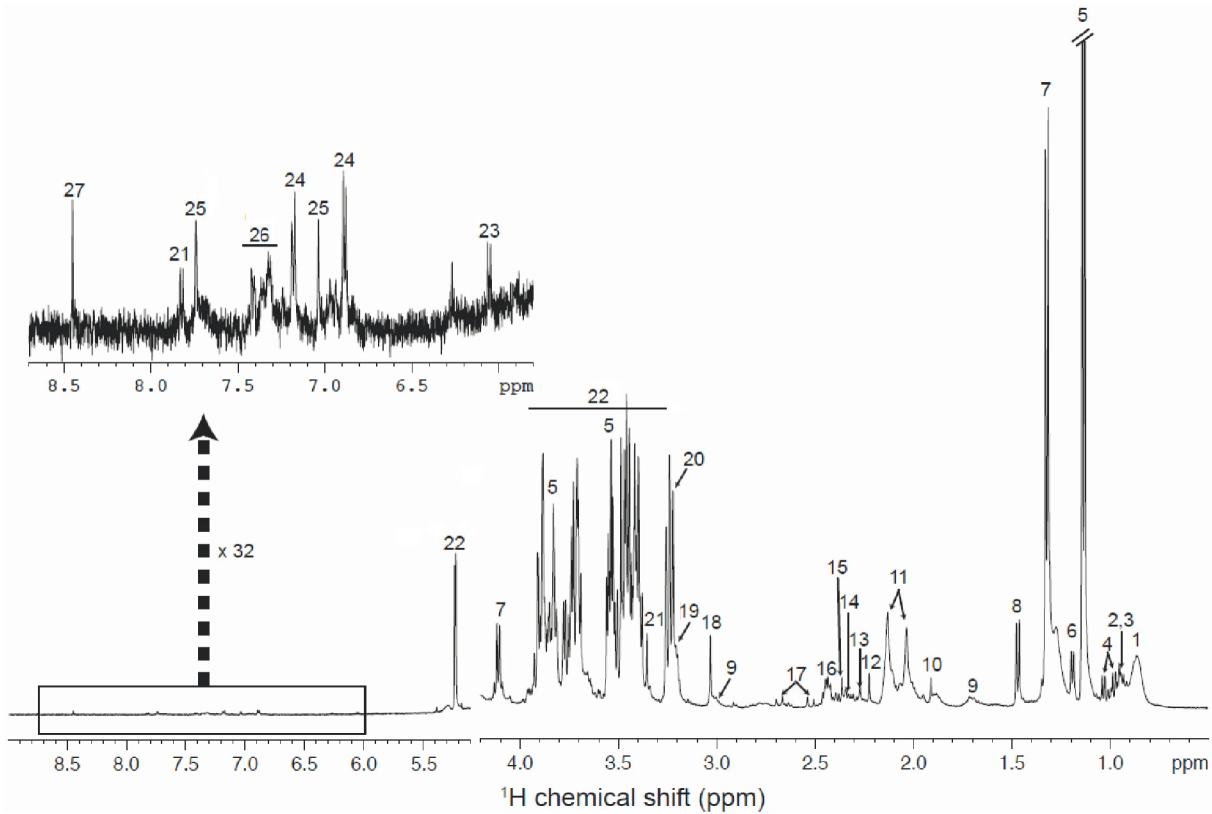


Fig 1. ¹H CPMG NMR spectrum of serum sample from rats fed with the HFS+C diet. Assignments: 1. lipids; 2. isoleucine; 3. leucine; 4. valine; 5. propylene glycol; 6. β-hydroxybutyrate; 7. lactate; 8. alanine; 9. lysine; 10. acetate; 11. glycoproteins (acetyl); 12. acetoacetate; 13. unknown; 14. glutamate; 15. pyruvate; 16. glutamine; 17. citrate; 18. creatine; 19. choline; 20. phosphocholine/glycerophosphocholine; 21. methanol; 22. alpha-glucose and beta-glucose; 23. cytidine; 24. tyrosine; 25. histidine; 26. phenylalanine; 27. formate.

doi:10.1371/journal.pone.0135948.g001

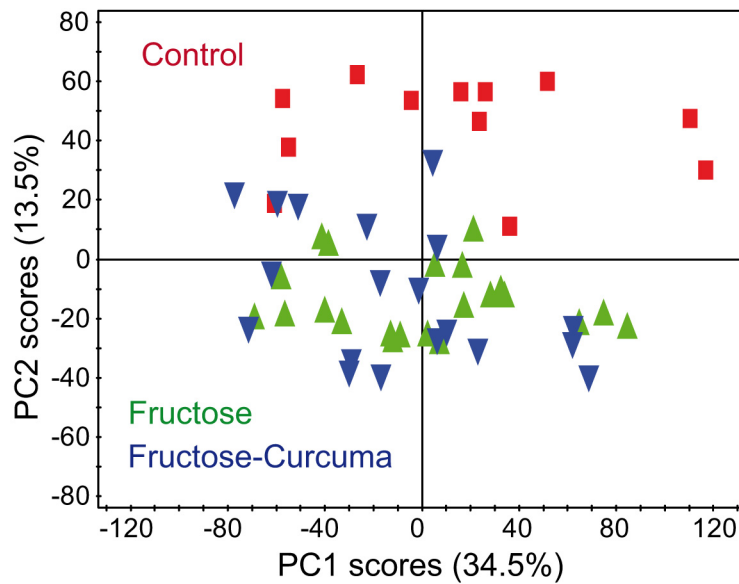


Fig 2. PCA score plot of the serum samples from Control, HFS and HFS+C groups.

doi:10.1371/journal.pone.0135948.g002

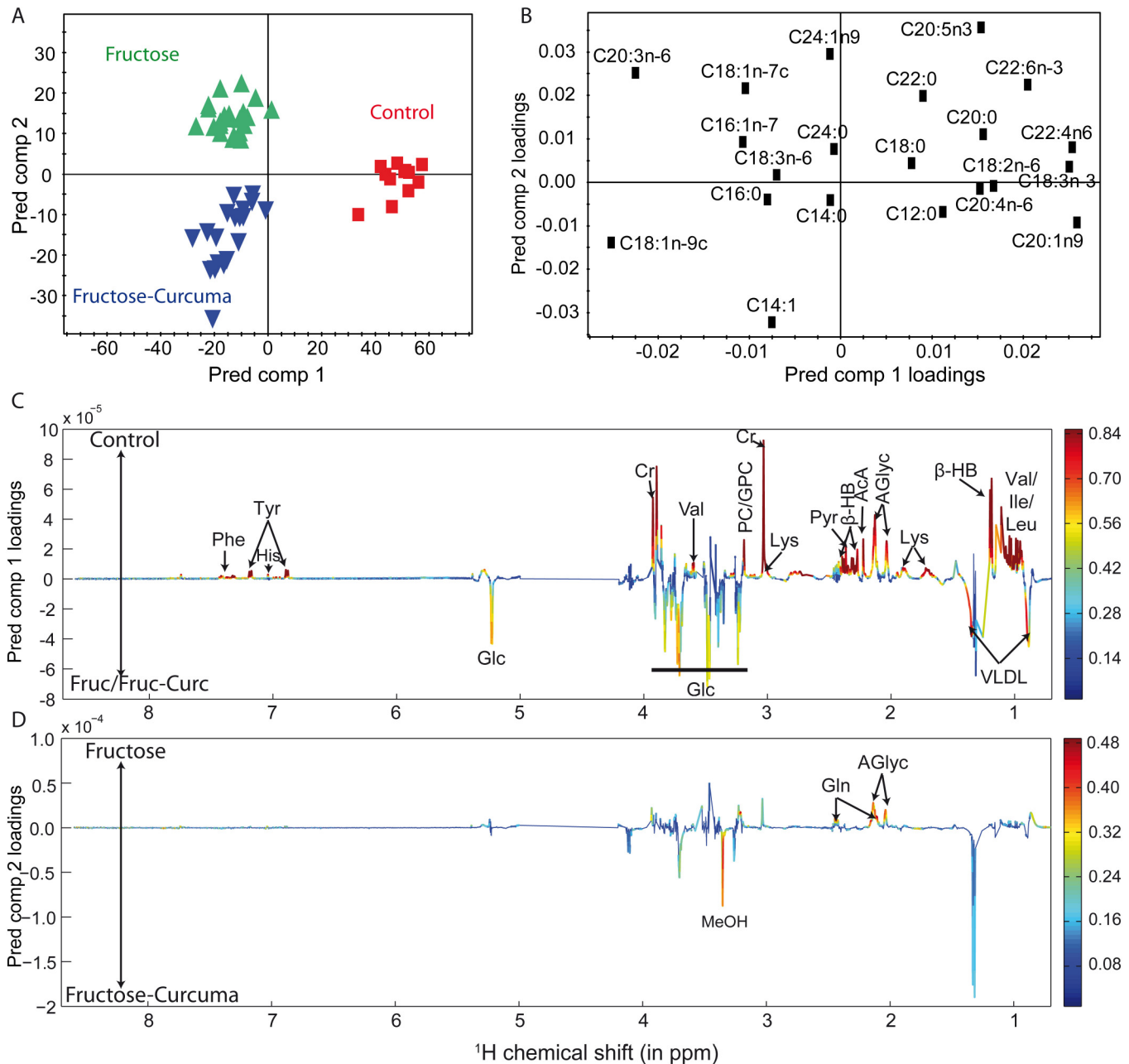


Fig 3. OPLS-DA score and loadings plots. (A) OPLS-DA score plot representing the 54 samples in the Tpred 1 vs Tpred 2 plane. (B, C-D) OPLSDA loadings plot representing the weights of the relative fatty acid contents and the NMR signals, respectively, along the two predictive components derived from OPLS-DA model of serum samples obtained from controls, HFS and HFS+C groups. The line variation (C, D) corresponds to model covariance derived from the mean-centered model, whereas the color map corresponds to model correlation derived from the unit-variance model.

doi:10.1371/journal.pone.0135948.g003

fatty acid quantification in the X-matrix when we compared the PCA models built with or without replication (see [S2 Fig](#)).

Instead, a 2 predictive (Tpred) and 4 orthogonal components OPLS-DA model with a p-value of 1.2×10^{-3} ($R^2Y = 0.64$, $Q^2Y = 0.46$) enabled a clear discrimination between the three studied groups. The first predictive component was related to the diet-induced metabolic variations ([Fig 3A](#)) involving a decrease of several amino acids (phenylalanine, tyrosine, histidine,

valine, lysine, isoleucine, leucine), pyruvate, acetoacetate, β -hydroxybutyrate, creatine, phosphocholine and glycerophosphocholine, alpha-linoleic (18:2n-6), alpha-linolenic (C18:3n-3), gondoic (C20:1n-9), arachidonic (C20:4n-6), adrenic (C22:4n-6), docosahexaenoic (C22:6n-3) acids associated with an increase of glucose, very low density lipoproteins (VLDL), palmitoleic (C16:1n-7), oleic (C18:1n-9) and dihomo-gamma-linolenic (C20:3n-6) acids in HFS and HFS+C groups (Fig 3B). The second predictive component reflects the curcuma-induced metabolic variations involving a decrease of glutamine, acetylated glycoproteins, eicosopentaenoic (C20:5n-3), docosahexaenoic (C22:6n-3), nervonic (C24:1n-9) acids combined with an increase of methanol, oleic (C18:1n-9) and myristoleic (C14:1n-5) acids. The Y-permutation model validated the robustness of the model and confirmed that the observed metabolic variations were not randomly induced (see S3 Fig). The relative discriminant metabolite variations are reported in Table 5.

Discussion

Effects of HFS and HSF+C diets on the metabolism

Our discussion will focus on the metabolic variations induced by the curcuma supplement extract. However, to put this in perspective, we first analyzed the metabolic variations common to HFS and HFS+C groups.

Classical tests. Interestingly, compared to HFS group, rats having received extract of curcuma tended to have a lower insulin level and higher concentration of triglycerides in the serum. These observations points towards specific but incomplete protective effects of curcumin for insulinemia and indirectly for fatty liver disease, as the most elevated triglyceride level observed in the HFS+C group may indicate a release of fat from the liver. Regulation of glucose and cholesterol, previously reported in the literature for diets with curcuma complement, was not observed [24,25]. This is most likely due to the much lower dosage (1 mg/kg body weight/day) of curcuminoids that we used, 1 to 2 order of magnitude less compared to previous studies, which led to no detectable curcumin in the serum [24,26]. Note that our dosage was selected to correspond to the habitual intake of curcuminoids in the Asian population as recommended in the joint report of the Food and Agriculture Organization and the World Health Organization on food additives [27].

Oxidative stress. Our results (Table 3) associated HFS groups rats with an increase in lipid peroxidation and a decrease in TAC in serum, suggesting increased in ROS production and/or a weakening of the antioxidant system defenses. Fructose-induced hyperglycemia and high plasma levels of triglycerides could promote increasing generation of ROS and reducing the antioxidant defense status [28].

The oral administration of curcuma extract did not counteract the oxidative stress induced by the HFS diet, in contrast to previous studies, which have shown that CL powder by itself, and its major bioactive component curcumin, would protect against oxidative stress thanks to a radical-trapping ability as chain-breaking antioxidant [29]. As seen above, the discrepancy may be explained by the dose of curcuminoids and the composition of diet used here.

NMR and GC/MS discrimination between Control and HFS/HFS+C groups

Table 5 reports the observed metabolite modulations with respect to the diets of our animal model. High-level of glucose and VLDL are well-characterized effects of a HFS diet [6,22]. The increase in the availability of gluconeogenic substrates have been suggested to be the major cause of fasting hyperglycemia in HFS-fed rats [30]. An increase in the production of VLDL in

Table 5. Significantly differential metabolites in the rat serum of control, HFS and HFS+C group.

metabolites	Changes in HFS (vs Controls)	Changes in HFS+C (vs Controls)	Changes in HFS+C (vs HFS)
Acetoacetate	↓ 1.43	↓ 1.29	
β-hydroxybutyrate	↓ 1.45	↓ 1.39	
Creatine	↓ 1.53	↓ 1.82	
Glucose	↑ 1.37	↑ 1.31	
Glutamine			↓ 1.13
Glycoproteins (acetyl)		↓ 1.12	↓ 1.13
Histidine	↓ 1.30	↓ 1.44	
Isoleucine	↓ 1.36	↓ 1.25	
Leucine	↓ 1.21	↓ 1.17	
Lysine	↓ 1.17	↓ 1.13	
Methanol		↑ 1.55	↑ 1.40
Phenylalanine	↓ 1.85	↓ 1.43	
Phosphocholine/ Glycerophosphocholine	↓ 1.21	↓ 1.25	
Pyruvate	↓ 1.23	↓ 1.14	
Tyrosine	↓ 1.68	↓ 1.77	
Valine	↓ 1.38	↓ 1.33	
VLDL	↑ 1.51	↑ 1.55	
Fatty acids			
C14:1n-5 Myristoleic acid		↑ 2.54	↑ 2.20
C16:1n-7 Palmitoleic acid	↑ 1.45	↑ 1.30	
C18:1n-9 Oleic acid	↑ 2.28	↑ 2.78	↑ 1.22
C18:2n-6 Linoleic acid	↓ 1.30	↓ 1.28	
C18:3n-3 alpha Linolenic acid	↓ 3.36	↓ 4.43	
C20:1n-9 Gondoic acid	↓ 4.64	↓ 3.33	
C20:3n-6 Dihomo gamma linolenic acid	↑ 4.18	↑ 3.29	
C20:4n-6 Arachidonic acid	↓ 1.24	↓ 1.30	
C20:5n-3 Eicosopentaenoic acid		↓ 5.55	↓ 3.69
C22:4n-6 Adrenic acid	↓ 3.90	↓ 7.55	
C22:6n-3 Docosahexaenoic acid	↓ 1.49	↓ 1.55	↓ 2.31
C24:1n-9 Nervonic acid			↓ 1.38

The serum metabolites that contributed significantly to the discrimination between the different diets in the OPLS-DA model from the ¹H NMR data. ↑ (or ↓) denotes the relative increased (or decreased), followed by fold change in metabolite level (p < 0.05). The levels were calculated from relative intensities of ¹H NMR spectra following spectral normalization.

doi:10.1371/journal.pone.0135948.t005

animal of high-fructose feeding may be driven by IR [31], increased triglyceride flux and hepatic inflammation [32], and decreased clearance [33]. The use of choline or phosphatidylcholine for VLDL secretion could explain the depletion of phosphocholine and glycerophosphocholine [34]. Furthermore, this depletion also suggests a possible involvement of gut microbiota, which in high fat diet-induced IR mice was found to convert dietary choline into methylamines with an increased level of methylamines urinary excretion, thereby reducing the bioavailability of choline [35].

Considering that the blood samples were drawn after a fasting period, it is not surprising that the ¹H NMR spectrum comparison between controls and HFS groups revealed a substantial perturbation of key metabolites related to energy production. Indeed, HFS rat groups had

lower ketone bodies, pyruvate, creatine, and amino acids. Pyruvate, creatine and glycoproteins were reported in a recent NMR metabolomics studies to be more abundant in lean vs. obese pigs sera [36]. The level of decreasing pyruvate in HFS groups suggests an enhancement of the lipogenesis observed in fructose consumption [37].

The lower level of creatine in the HFS and HFS+C groups may be linked to the depletion of choline, as the deficiency of this latter increases the utilization of S-adenosylmethionine for phosphatidylcholine synthesis, making it less available for the synthesis of creatine [38]. Moreover, creatine has an antioxidant activity and its reduction could be related to the oxidative stress measured in HFS groups [39].

More abundant acetoacetate and β -hydroxybutyrate in the control serum at concentration detectable by ^1H NMR is not surprising due to the several hours of fasting imposed before sacrifice. While the role of ketone bodies (KB) besides being energy carriers is still being investigated [40], the reduced concentration of KB in HFS groups correlates well with the inhibition of ketogenesis by insulinemia [41] and with the higher glucose concentration observed in HFS groups. Given that IR suppresses hepatic FA catabolism and stimulates hepatic lipogenesis and FA esterification [42], HFS diet that leads to IR may cause a greater fractional esterification of FA and a lower beta-oxidation of KB [43].

We also observed a lower relative concentration of several amino acids: phenylalanine, tyrosine, histidine, lysine, and the branched chain amino acids (BCAA) isoleucine, leucine, valine in both HFS groups compared to controls. This is consistent with previously reported studies [13,44], suggesting a perturbation of the energy metabolism. Under hyperinsulinemia conditions or in the presence of FA-induced IR, measured plasma amino acid concentrations have been observed to decline, suggesting lower rates of protein breakdown and protein synthesis [45,46]. Furthermore, there are conflicting data concerning the role of BCAA: a study reported that supplementation of a high fat diet in rats with BCAA contributed to development of IR [47], while another one has demonstrated that higher BCAA intake in humans is inversely associated with prevalence of overweight and obesity [48]. Moreover, most of these amino acids are gluconeogenic and may contribute to elevated rate of gluconeogenesis as reported in high fructose diet [30], the exception being leucine and lysine, which play a protective role in the IR, improving insulin sensitivity [49] and inhibiting protein glycation, respectively [50].

Out of the twenty-one fatty acids quantified in this study, twelve have their concentration altered significantly between controls and HFS rats. The serum FA profile in HFS-fed rats was characterized by a higher proportion of MUFA and by a lower proportion of PUFA, as already observed in our previous study [22]. This behavior corresponds in general to a higher oxidation activity as detected in the HFS groups. More specifically, an increased activity of $\Delta 9\text{D}$ observed in HFS group, coupled to the increase in triglycerides could represent an initial cellular defense against lipotoxicity in response to acute HFS diet, for the sequestering of palmitic acid into triglycerides [51]. The decrease of n-3 PUFA, alpha-linolenic acid (18:3 n-3), EPA (20:5n-3) and DHA (22:6 n-3) induced by the HFS diet could be involved in early processes that lead to IR [52].

Specific effects of curcuma dietary supplement on the metabolism

According to the OPLS-DA loadings (Fig 3B and 3D), alterations of some FAs, an increase of methanol and a decrease of glutamine and glycoproteins were observed in the HFS+C group compared to the HFS one.

Fatty acids. The presence of curcuminoids in the diet induced some noticeable alterations of the FA metabolism with respect to the HFS diet: a further increase in some MUFA (myristoleic acid, oleic acid, nervonic acid) and a further decrease in eicosapentaenoic and docosahexaenoic acid suggesting that the metabolism of the n-3 PUFAs was affected. Curcumin is a

non-specific and non-competitive inhibitor of the desaturases in rat liver microsomes [53], which could explain our results. There is a consensus on the existence of competition among fatty acids of the n-3 and n-6 families for desaturation and chain elongation, 18:3 n-3 being a better substrate for $\Delta 6$ desaturase than 18:2 n-6 [54]. The presence and increase of 14:1n-5 (myristoleic acid) provided evidence that 14:0 (myristic acid) was also converted by stearoyl-CoA desaturase. Associated with the increase of 18:1n-9, it suggests a stimulation of stearoyl-CoA desaturase activity by curcumin. Thus, as reported above, the raise in 18:1n-9 could lead to the accumulation of triglycerides that rescues C16:0-induced apoptosis by channelling C16:0 into triglycerides and away from pathways introducing to apoptosis [52]. The level of nervonic acid (24:1n-9) was significantly depressed by addition of CL extract to the diet. This FA is normally present only in sphingomyelin, a major component located mostly in the outer layer of the plasma membrane and plays a role in maintaining the membrane in a more rigid state [55]. In overweight and obese female erythrocytes membranes, 24:1n-9 was found increased and correlated with decreased membrane fluidity [56]. Given that the IR and the decrease of membrane fluidity are associated [57], curcumin could offer protection from the rigidifying of the membrane by decreasing the level of 24:1n-9 in acting on the elongation steps of its synthesis. Further experiments are required to elucidate this finding.

Methanol. Intriguingly, we observed a higher level of methanol in HFS+C group compared to HFS group. Although generally endogenously produced from gut microbiota, methanol is more likely to be generated here as a product of mammalian intermediary metabolism [58]. The methanol formed would be oxidized sequentially to formaldehyde, then to formic acid and finally to carbon dioxide. This occurs mainly in the liver, mediated by alcohol dehydrogenase (ADH) and aldehyde dehydrogenase (ALDH) [59]. In rats, catalase is also a significant pathway of methanol metabolism [60]. Fructose decreases catalase-dependent alcohol oxidation due to the inhibition of H_2O_2 generation via peroxisomal beta-oxidation of fatty acids by decreasing ATP and the NAD/NADH ratio [61]. Thus, in HFS diets, the oxidation of methanol should be mediated predominantly via ADH. In this work, the curcuma-free oral vehicle and the hydroalcoholic extract of curcuma (methanol-free) administered in aqueous suspension daily to the rats contained 2% of ethanol, which is able to inhibit the oxidation of methanol by ADH [62]. Indeed, this latter has a better affinity and specificity for ethanol than for methanol [63], thus ethanol is preferentially metabolised by ADH. In addition, it has been shown that fructose increases the rate of ethanol metabolism in both animals and man [64,65]. Since HFS and HFS+C groups received the same amount of ethanol, the higher level of methanol observed in the HFS+C group can stem from the curcuminoids present in the turmeric extract. Interestingly, previous studies have shown that curcumin is a substrate of ADH and a preparation of curcumin impaired the ethanol oxidation via ADH in humans [66]. Thus, the increase in methanol level observed in HFS+C group might be explained by an inhibition of methanol (alcohol) elimination in the liver with a concomitant constant endogenous production.

Glutamine and glycoproteins. An increased level of glutamine and glycoproteins were observed in the HFS group compared to HFS+C one. This suggests alterations in glutamine metabolism as observed in type II diabetics [67] and a possible activation of the hexosamine biosynthesis pathway (HBP). The HBP is a minor branch from glycolysis pathway from which fructose-6-phosphate (F-6-P) amidotransferase (GFAT) forms glucosamine-6-phosphate (GlcN-6-P) [68]. Subsequent enzymatic reactions metabolize GlcN-6-P to UDP-N-acetylglucosamine (UDP-GlcNAc), the major end product of the HBP [69]. Previous studies have demonstrated that HBP can play a role in IR, given that many proteins involved in insulin signal transduction (as insulin receptor substrate, IRS) or in glucose transporter (GLUT) are subject to O-GlcNAcylation [70]. Moreover, glutamine is a key inducer of HBP flux by providing the

amide group for the formation of hexosamines and it is required in desensitization of insulin-responsive glucose transport system [71]. Thus, the hyperglycemia seen in HFS group could increase the glucose availability through the HBP leading to accumulation of glycoproteins and leading to IR. On the other hand, despite the extract of curcuma used here not normalising glycemia, a lower level of glycoproteins was observed in the HFS+C group. This is in agreement with a study showing that oral administration of tetrahydrocurcumin (a metabolite of curcumin) to diabetic rats decreased the level of plasma glycoproteins [72].

Conclusion

A view of the metabolic changes in an animal model fed with high fructose and saturated fatty acid diet, as long as the effects of integration with the nutritional supplement *Curcuma longa* has been provided by NMR metabolomics and GC-MS lipidomics of the serum. While the observed and expected, diet-induced, metabolic disorders (insulin resistance) could not be countered by the nutritional supplement, elements have been discerned of a possible localized protection, notably at the liver level. Indeed, while perturbation of several energy-related metabolites (amino acids, ketonic bodies, creatine, pyruvate, glucose, VLDL) have been observed in both animals fed with the high fructose and saturated fatty acid diets, despite *Curcuma longa* dietary supplementation, specific biomarkers could be associated to this latter setup. Particularly, a depression of the alcohol oxidation, detected through an enhanced concentration of methanol, and a possible activation of the hexosamine biosynthesis pathway, consistent with a reduction of glutamine and glycoprotein levels. Both these two effects point towards a modified liver function. Further biomarkers of the curcuminoid enriched diet were a significant alteration of the concentration of long chain unsaturated fatty acids: C20:5n-3, C22:6n-3 and C24:1n-9. The variation in the concentration in this latter is a specific effect of the nutritional supplement, as it is not observed in the high fructose and saturated fatty acid diet groups, and is suggestive of a cellular enhanced response to the membrane rigidification associated to insulin resistance. All of these points to possible specific and local, rather than systemic, protective effects of *Curcuma longa*, and further studies are underway to clarify this issue.

Supporting Information

S1 Fig. ¹H NOESY NMR spectrum of serum sample from rat fed with a HFS diet supplemented with curcuma extract. Assignments: 1, lipids; 2, isoleucine; 3, leucine; 4, valine; 5, propylene glycol; 6, β-hydroxybutyrate; 7, lipids; 8, lactate; 9, alanine; 10, lipids; 11, lysine; 12, lipids; 13, acetate; 14, glycoproteins (acetyl); 15, acetoacetate; 16, unknown; 17, glutamate; 18, pyruvate; 19, glutamine; 20, citrate; 21, lipids; 22, creatine; 23, choline; 24, phosphocholine/glycerophosphocholine; 25, methanol; 26, alpha-glucose and beta-glucose; 27, lipids; 28, cytidine; 29, tyrosine; 30, histidine; 31, phenylalanine; 32, formate.
(PDF)

S2 Fig. PC1 vs PC2 score plot of 28 serum samples. For this analysis, one aliquot per sample was considered.
(PDF)

S3 Fig. Validation plot. Model validation resulting from 999 permutations, demonstrating the model robustness, because model R2 and Q2 values were significantly higher than random model ones.
(PDF)

S1 Table. Assignment of ^1H and ^{13}C NMR signals of metabolites. (PDF)

Acknowledgments

The authors thank Mr. Nicolas Vidal and Dr. Pierre Stocker for performing the analysis of oxidative stress.

Author Contributions

Conceived and designed the experiments: FT LS. Performed the experiments: FT LS LT ZR. Analyzed the data: FT LS AH SC. Contributed reagents/materials/analysis tools: FT LS ZR LT VD. Wrote the paper: FT LS SC. Supervised all areas of the research: AH SC.

References

1. Rippe JM, Angelopoulos TJ. Sucrose, High-Fructose Corn Syrup, and Fructose, Their Metabolism and Potential Health Effects: What Do We Really Know? *Adv Nutr*. 2013; 4: 236–245. doi: [10.3945/an.112.002824](https://doi.org/10.3945/an.112.002824) PMID: [23493540](https://pubmed.ncbi.nlm.nih.gov/23493540/)
2. Malik VS, Schulze MB, Hu FB. Intake of sugar-sweetened beverages and weight gain: a systematic review. *Am J Clin Nutr*. 2006; 84: 274–288. PMID: [16895873](https://pubmed.ncbi.nlm.nih.gov/16895873/)
3. Astrup A, Finer N. Redefining type 2 diabetes: “diabesity” or “obesity dependent diabetes mellitus”? *Obes Rev*. 2000; 1: 57–59. PMID: [12119987](https://pubmed.ncbi.nlm.nih.gov/12119987/)
4. Balkau B, Charles MA, Drisvholm T, Borch-Johnsen K, Wareham N, Yudkin JS, et al. Frequency of the WHO metabolic syndrome in European cohorts, and an alternative definition of an insulin resistance syndrome. *Diabetes Metab*. 2002; 28: 364–376. PMID: [12461473](https://pubmed.ncbi.nlm.nih.gov/12461473/)
5. Griffin ME, Marcucci MJ, Cline GW, Bell K, Barucci N, Lee D, et al. Free fatty acid-induced insulin resistance is associated with activation of protein kinase C theta and alterations in the insulin signaling cascade. *Diabetes*. 1999; 48: 1270–1274. PMID: [10342815](https://pubmed.ncbi.nlm.nih.gov/10342815/)
6. Girard A, Madani S, El Boustani ES, Belleville J, Prost J. Changes in lipid metabolism and antioxidant defense status in spontaneously hypertensive rats and Wistar rats fed a diet enriched with fructose and saturated fatty acids. *Nutrition*. 2005; 21: 240–248. PMID: [15723754](https://pubmed.ncbi.nlm.nih.gov/15723754/)
7. Evans JL, Goldfine ID, Maddux BA, Grodsky GM. Are oxidative stress-activated signaling pathways mediators of insulin resistance and beta-cell dysfunction? *Diabetes* 2003; 52: 1–8. PMID: [12502486](https://pubmed.ncbi.nlm.nih.gov/12502486/)
8. Araújo CC, Leon LL. Biological activities of *Curcuma longa* L. *Mem. Inst Oswaldo Cruz*. 2001; 96: 723–728. PMID: [11500779](https://pubmed.ncbi.nlm.nih.gov/11500779/)
9. Gupta SC, Patchva S, Aggarwal BB. Therapeutic roles of curcumin: lessons learned from clinical trials. *AAPS J*. 2013; 15: 195–218. doi: [10.1208/s12248-012-9432-8](https://doi.org/10.1208/s12248-012-9432-8) PMID: [23143785](https://pubmed.ncbi.nlm.nih.gov/23143785/)
10. Na LX, Zhang YL, Li Y, Liu LY, Li R, Kong T, et al. Curcumin improves insulin resistance in skeletal muscle of rats. *Nutr Metab Cardiovasc Dis*. 2011; 21: 526–533. doi: [10.1016/j.numecd.2009.11.009](https://doi.org/10.1016/j.numecd.2009.11.009) PMID: [20227862](https://pubmed.ncbi.nlm.nih.gov/20227862/)
11. Neyrinck AM, Alligier M, Memvanga PB, Névrumont E, Larondelle Y, Pr at V, et al. *Curcuma longa* extract associated with white pepper lessens high fat diet-induced inflammation in subcutaneous adipose tissue. *PloS one*. 2013; 8(11): e81252. doi: [10.1371/journal.pone.0081252](https://doi.org/10.1371/journal.pone.0081252) PMID: [24260564](https://pubmed.ncbi.nlm.nih.gov/24260564/)
12. Kim HJ, Kim JH, Noh S, Hur HJ, Sung MJ, Hwang JT, et al. Metabolomic analysis of livers and serum from high-fat diet induced obese mice. *J Proteome Res*. 2011; 10: 722–731. doi: [10.1021/pr100892r](https://doi.org/10.1021/pr100892r) PMID: [21047143](https://pubmed.ncbi.nlm.nih.gov/21047143/)
13. Shearer J, Duggan G, Weljie A, Hittel DS, Wasserman DH, Vogel HJ. Metabolomic profiling of dietary-induced insulin resistance in the high fat-fed C57BL/6J mouse. *Diabetes Obes Metab*. 2008; 10: 950–958. doi: [10.1111/j.1463-1326.2007.00837.x](https://doi.org/10.1111/j.1463-1326.2007.00837.x) PMID: [18215169](https://pubmed.ncbi.nlm.nih.gov/18215169/)
14. Lin S, Yang Z, Liu H, Tang L, Cai Z. Beyond glucose: metabolic shifts in responses to the effects of the oral glucose tolerance test and the high-fructose diet in rats. *Mol BioSyst*. 2011; 7: 1537–1548. doi: [10.1039/c0mb00246a](https://doi.org/10.1039/c0mb00246a) PMID: [21350749](https://pubmed.ncbi.nlm.nih.gov/21350749/)
15. Matthews DR, Hosker JP, Rudenski AS, Naylor BA, Treacher DF, Turner RC. Homeostasis model assessment: insulin resistance and beta-cell function from fasting plasma glucose and insulin concentrations in man. *Diabetologia*. 1985; 28: 412–419. PMID: [3899825](https://pubmed.ncbi.nlm.nih.gov/3899825/)

16. Masood A, Stark KD, Salem N. A simplified and efficient method for the analysis of fatty acid methyl esters suitable for large clinical studies. *J Lipid Res.* 2005; 46: 2299–2305. PMID: [16061957](#)
17. Clore JN, Harris PA, Li J, Azzam A, Gill R, Zuelzer W, et al. Changes in phosphatidylcholine fatty acid composition are associated with altered skeletal muscle insulin responsiveness in normal man. *Metab Clin Exp.* 2000; 49: 232–238. PMID: [10690951](#)
18. Huang D, Ou B, Hampsch-Woodill M, Flanagan JA, Prior RL. High-throughput assay of oxygen radical absorbance capacity (ORAC) using a multichannel liquid handling system coupled with a microplate fluorescence reader in 96-well format. *J Agric Food Chem.* 2002; 50: 4437–4444. PMID: [12137457](#)
19. Bax A, Davis DG. MLEV-17-based two-dimensional homonuclear magnetization transfer spectroscopy. *J Magn Reson.* 1985; 65: 355–360.
20. Bodenhausen G, Ruben DJ. Natural abundance nitrogen-15 NMR by enhanced heteronuclear spectroscopy. *Chem Phys Lett.* 1980; 69: 185–189.
21. Trygg J, Wold S. Orthogonal projections to latent structures (O-PLS). *J Chemom.* 2002; 16: 119–128.
22. Tranchida F, Tchiakpe L, Rakotoniaina Z, Deyris V, Ravion O, Hioi A. Long-term high fructose and saturated fat diet affects plasma fatty acid profile in rats. *J Zhejiang Univ Sci B.* 2012; 13: 307–317. doi: [10.1631/jzus.B1100090](#) PMID: [22467372](#)
23. D'Angelo G, Elmarakby AA, Pollock DM, Stepp DW. Fructose feeding increases insulin resistance but not blood pressure in Sprague-Dawley rats. *Hypertension.* 2005; 46: 806–811. PMID: [16157789](#)
24. Seo KI, Choi MS, Jung UJ, Kim HJ, Yeo J, Jeon S.M, et al. Effect of curcumin supplementation on blood glucose, plasma insulin, and glucose homeostasis related enzyme activities in diabetic db/db mice. *Mol Nutr Food Res.* 2008; 52: 995–1004. doi: [10.1002/mnfr.200700184](#) PMID: [18398869](#)
25. Patil TN, Srinivasan M. Hypocholesteremic effect of curcumin in induced hypercholesteremic rats. *Indian J Exp Biol.* 1971; 9: 167–169. PMID: [5092727](#)
26. Pongchaidecha A, Lailerd N, Boonprasert W, Chattipakorn N. Effects of curcuminoid supplement on cardiac autonomic status in high-fat-induced obese rats. *Nutrition.* 2009; 25: 870–878. doi: [10.1016/j.nut.2009.02.001](#) PMID: [19398300](#)
27. Joint Expert Committee of the Food and Agriculture Organization/World Health Organization Evaluation of certain food additives and contaminants. Sixty-first report of the Joint FAO/WHO Expert Committee on Food Additives. WHO Technical Report Series 922. Geneva. 2004.
28. Faure P, Rossini E, Lafond JL, Richard MJ, Favier A, Halimi S. Vitamin E improves the free radical defense system potential and insulin sensitivity of rats fed high fructose diets. *J Nutr.* 1997; 127: 103–107. PMID: [9040552](#)
29. Sreejayan N, Rao MNA, Priyadarsini KI, Devasagayamc TPA. Inhibition of radiation-induced lipid peroxidation by curcumin. *Int J Pharm.* 1997; 151: 127–130.
30. Thresher JS, Podolin DA, Wei Y, Mazzeo RS, Pagliassotti MJ. Comparison of the effects of sucrose and fructose on insulin action and glucose tolerance. *Am J Physiol Regul Integr Comp Physiol.* 2000; 279: R1334–1340. PMID: [11004002](#)
31. Taghibiglou C, Rashid-Kolvear F, Van Iderstine SC, Le-Tien H, Fantus IG, et al. Hepatic very low density lipoprotein-ApoB overproduction is associated with attenuated hepatic insulin signaling and overexpression of protein-tyrosine phosphatase 1B in a fructose-fed hamster model of insulin resistance. *J Biol Chem.* 2002; 277: 793–803. PMID: [11598116](#)
32. Tsai J, Zhang R, Qiu W, Su Q, Naples M, Adeli K. Inflammatory NF-kappaB activation promotes hepatic apolipoprotein B100 secretion: evidence for a link between hepatic inflammation and lipoprotein production. *Am J Physiol Gastrointest Liver Physiol.* 2009; 296: G1287–1298. doi: [10.1152/ajpgi.90540.2008](#) PMID: [19342510](#)
33. Hirano T, Mamo JC, Poapst ME, Kuksis A, Steiner G. Impaired very low-density lipoprotein-triglyceride catabolism in acute and chronic fructose-fed rats. *Am J Physiol.* 1989; 256: E559–565. PMID: [2705524](#)
34. Zeisel SH, Blusztajn JK. Choline and human nutrition. *Annu Rev Nutr.* 1994; 14: 269–296. PMID: [7946521](#)
35. Dumas ME, Barton RH, Toye A, Cloarec O, Blancher C, Rothwell A, et al. Metabolic profiling reveals a contribution of gut microbiota to fatty liver phenotype in insulin-resistant mice. *Proc Natl Acad Sci U S A.* 2006; 103: 12511–12516. PMID: [16895997](#)
36. He Q, Ren P, Kong X, Wu Y, Wu G, Li P, et al. Comparison of serum metabolite compositions between obese and lean growing pigs using an NMR-based metabonomic approach. *J Nutr Biochem.* 2012; 23: 133–139. doi: [10.1016/j.jnutbio.2010.11.007](#) PMID: [21429726](#)
37. Havel PJ. Dietary Fructose: Implications for Dysregulation of Energy Homeostasis and Lipid / Carbohydrate Metabolism. *Nutr Rev.* 2005; 63: 133–157. PMID: [15971409](#)

38. Schneider WJ, Vance DE. Effect of choline deficiency on the enzymes that synthesize phosphatidylcholine and phosphatidylethanolamine in rat liver. *Eur J Biochem.* 1978; 85: 181–187. PMID: [639815](#)
39. Sestili P, Martinelli C, Colombo E, Barbieri E, Potenza L, Sartini S, et al. Creatine as an antioxidant. *Amino acids.* 2011; 40: 1385–1396. doi: [10.1007/s00726-011-0875-5](#) PMID: [21404063](#)
40. Newman JC, Verdin E. Ketone bodies as signaling metabolites. *Trends Endocrinol Metab.* 2014; 25: 42–52. doi: [10.1016/j.tem.2013.09.002](#) PMID: [24140022](#)
41. Mahendran Y, Vangipurapu J, Cederberg H, Stancáková A, Pihlajamäki J, Soininen P, et al. Association of ketone body levels with hyperglycemia and type 2 diabetes in 9,398 Finnish men. *Diabetes.* 2013; 62: 3618–3626. doi: [10.2337/db12-1363](#) PMID: [23557707](#)
42. Fukuda N, Azain MJ, Ontko JA. Altered hepatic metabolism of free fatty acids underlying hypersecretion of very low density lipoproteins in the genetically obese Zucker rats. *J Biol Chem.* 1982; 257: 14066–14072. PMID: [7142195](#)
43. Lê K, Ith M, Kreis R, Faeh D. Fructose overconsumption causes dyslipidemia and ectopic lipid deposition in healthy subjects with and without a family history of type 2 diabetes. *Am J Clin Nutr.* 2009; 1760–1765. doi: [10.3945/ajcn.2008.27336](#) PMID: [19403641](#)
44. Zhang X, Wang Y, Hao F, Zhou X, Han X. Human serum metabolomic analysis reveals progression axes for glucose intolerance and insulin resistance statuses. *J Proteome Res.* 2009; 8: 5188–5195. doi: [10.1021/pr900524z](#) PMID: [19697961](#)
45. Castellino P, Luzi L, Simonson DC, Haymond M, DeFronzo RA. Effect of insulin and plasma amino acid concentrations on leucine metabolism in man. Role of substrate availability on estimates of whole body protein synthesis. *J Clin Invest.* 1987; 80: 1784–1793. PMID: [3316280](#)
46. Katsanos CS, Aarsland A, Cree MG, Wolfe RR. Muscle protein synthesis and balance responsiveness to essential amino acids ingestion in the presence of elevated plasma free fatty acid concentrations. *J Clin Endocrinol Metab.* 2009; 94: 2984–2990. doi: [10.1210/jc.2008-2686](#) PMID: [19454587](#)
47. Newgard CB, An J, Bain JR, Muehlbauer MJ, Stevens RD, Lien LF, et al. A branched-chain amino acid-related metabolic signature that differentiates obese and lean humans and contributes to insulin resistance. *Cell Metab.* 2009; 9: 311–326. doi: [10.1016/j.cmet.2009.02.002](#) PMID: [19356713](#)
48. Qin L, Xun P, Bujnowski D, Daviglius ML, Horn L, Van Stamler J, et al. Higher Branched-Chain Amino Acid Intake Is Associated with a Lower Prevalence of Being Overweight or Obese in Middle-Aged East Asian and Western Adults. *J Nutr.* 2011; 141: 249–254. doi: [10.3945/jn.110.128520](#) PMID: [21169225](#)
49. Binder E, Bermúdez-Silva FJ, André C, Elie M, Romero-Zerbo SY, Leste-Lasserre T, et al. Leucine supplementation protects from insulin resistance by regulating adiposity levels. *PloS one.* 2013; 8: e74705. doi: [10.1371/journal.pone.0074705](#) PMID: [24086364](#)
50. Sensi M, De Rossi MG, Celi FS, Cristina A, Rosati C, Perrett D, et al. D-lysine reduces the non-enzymatic glycation of proteins in experimental diabetes mellitus in rats. *Diabetologia.* 1993; 36: 797–801. PMID: [8405749](#)
51. Listenberger LL, Han X, Lewis SE, Cases S, Farese RV, Ory DS, et al. Triglyceride accumulation protects against fatty acid-induced lipotoxicity. *Proc Natl Acad Sci U S A.* 2003; 100: 3077–3082. PMID: [12629214](#)
52. Ghafoorunissa, Ibrahim A, Rajkumar L, Acharya V. Dietary (n-3) long chain polyunsaturated fatty acids prevent sucrose-induced insulin resistance in rats. *J Nutr.* 2005; 135: 2634–2638. PMID: [16253960](#)
53. Kawashima H, Akimoto K, Jareonkitmongkol S, Shirasaka N, Shimizu S. Inhibition of rat liver microsomal desaturases by curcumin and related compounds. *Biosci Biotechnol Biochem.* 1996; 60: 108–110. PMID: [8824830](#)
54. Brenner RR, Peluffo RO. Effect of saturated and unsaturated fatty acids on the desaturation in vitro of palmitic, stearic, oleic, linoleic, and linolenic acids. *J Biol Chem.* 1966; 241: 5213–5219. PMID: [5927998](#)
55. Candiloros H, Zeghari N, Ziegler O, Donner M, Drouin P. Hyperinsulinemia is related to erythrocyte phospholipid composition and membrane fluidity changes in obese nondiabetic women. *J Clin Endocrinol Metab.* 1996; 81: 2912–2918. PMID: [8768851](#)
56. Cazzola R, Rondanelli M, Russo-Volpe S, Ferrari E, Cestaro B. Decreased membrane fluidity and altered susceptibility to peroxidation and lipid composition in overweight and obese female erythrocytes. *J Lipid Res.* 2004; 45: 1846–1851. PMID: [15231850](#)
57. Tong P, Thomas T, Berrish T, Humphriss D, Barriocanal L, Stewart M, et al. Cell membrane dynamics and insulin resistance in non-insulin-dependent diabetes mellitus. *Lancet.* 1995; 345: 357–358. PMID: [7845118](#)
58. Axelrod J, Daly J. Pituitary gland: enzymic formation of methanol from S-adenosylmethionine. *Science.* 1965; 150: 892–893. PMID: [5835789](#)
59. Tephly TR. The toxicity of methanol. *Life Sci.* 1991; 48: 1031–1041. PMID: [1997785](#)

60. Handler JA, Thurman RG. Hepatic ethanol metabolism is mediated predominantly by catalase-H₂O₂ in the fasted state. *FEBS Lett.* 1988; 238: 139–141. PMID: [3169246](#)
61. Woods HF, Eggleston LV, Krebs HA. The cause of hepatic accumulation of fructose 1-phosphate on fructose loading. *Biochem J.* 1970; 119: 501–510. PMID: [5500310](#)
62. Haffner HT, Graw M, Besserer K, Stränger J. Curvilinear increase in methanol concentration after inhibition of oxidation by ethanol: significance for the investigation of endogenous methanol concentration and formation. *Int J Legal Med.* 1998; 111: 27–31. PMID: [9457535](#)
63. Julià P, Farrés J, Parés X. Characterization of three isoenzymes of rat alcohol dehydrogenase. Tissue distribution and physical and enzymatic properties. *Eur J Biochem.* 1987; 162: 179–189. PMID: [3816781](#)
64. Tygstrup N, Winkler K, Lundquist F. the Mechanism of the Fructose Effect on the Ethanol Metabolism of the Human Liver. *J Clin Invest.* 1965; 44: 817–830. PMID: [14276139](#)
65. Scholz R, Nohl H. Mechanism of the stimulatory effect of fructose on ethanol oxidation in perfused rat liver. *Eur J Biochem.* 1976; 63: 449–458. PMID: [1261556](#)
66. Sasaki H, Sunagawa Y, Takahashi K, Imaizumi A, Fukuda H, Hashimoto T, et al. Innovative preparation of curcumin for improved oral bioavailability. *Biol Pharm Bull.* 2011; 34: 660–665. PMID: [21532153](#)
67. Stumvoll M, Perriello G, Nurjhan N, Bucci A, Welle S, Jansson PA, et al. Glutamine and alanine metabolism in NIDDM. *Diabetes.* 1996; 45: 863–68. PMID: [8666134](#)
68. Kornfeld S, Kornfeld R, Neufeld EF, O'Brien PJ. The feedback control of sugar nucleotide biosynthesis in liver. *Proc Natl Acad Sci U S A.* 1964; 52: 371–379. PMID: [14206604](#)
69. Lubas WA, Frank DW, Krause M, Hanover JA. O-Linked GlcNAc transferase is a conserved nucleocytoplasmic protein containing tetratricopeptide repeats. *J Biol Chem.* 1997; 272: 9316–9324. PMID: [9083068](#)
70. Patti ME, Virkamäki A, Landaker EJ, Kahn CR, Yki-Järvinen H. Activation of the hexosamine pathway by glucosamine in vivo induces insulin resistance of early postreceptor insulin signaling events in skeletal muscle. *Diabetes.* 1999; 48: 1562–1571. PMID: [10426374](#)
71. Marshall S, Bacote V, Traxinger RR. Discovery of a metabolic pathway mediating glucose-induced desensitization of the glucose transport system. Role of hexosamine biosynthesis in the induction of insulin resistance. *J Biol Chem.* 1991; 266: 4706–4712. PMID: [2002019](#)
72. Pari L, Murugan P. Changes in glycoprotein components in streptozotocin-nicotinamide induced type 2 diabetes: influence of tetrahydrocurcumin from *Curcuma longa*. *Plant Foods Hum Nutr.* 2007; 62: 25–29. PMID: [17226069](#)